Available free online at www.medjchem.com

Mediterranean Journal of Chemistry

Mediterranean Journal of Chemistry **2020**, 10(4), 319-334

Rotational barrier and electron-withdrawing substituent effects: Theoretical study of π-conjugation in *para*-substituted anilines

Ali Hussain Yateem

Department of Chemistry, College of Science, University of Bahrain, P. O. Box 32038, Sakhir, Kingdom of Bahrain

Abstract: The rotational barrier RB around C–NH_2 bond between the minimum and maximum states of 84 electron-withdrawing groups at *para*-position in aniline were studied at the density functional ωB97X-D/6-31G** level. The rotational barrier was found to correlate strongly with shortening of the C–NH_2 bond, increase of flattening of NH_2 group, decrease in negative natural charge on amino nitrogen, increase in minimum ionization potential around lone pair of amino nitrogen, increase in maximum (positive) electrostatic potential on amino hydrogens, increase in NH_2 stretching frequencies, and increase in stabilization energy. The rotational barrier was also found to correlate well with empirical pK_a and Hammett σ_p constants. The rotational barrier is shown to be a reliable quantum mechanical approach to measure π-conjugation in para-substituted anilines. Based on RB a quantitative scale is constructed for the ability of electron-withdrawing substituents to resonate with aniline. A quinone-like structure has been proposed for stronger electron-withdrawing substituents where an extension of resonance stabilization requires the simultaneous presence of electron donor (NH_2) and electron-withdrawing groups.

Keywords: Rotational barrier; substituent effects; electron-withdrawing groups; para-substituted anilines.

1. Introduction

Empirical Hammett parameters are used to describe substituent effects in various aromatic systems [1,2]. Several physical and chemical parameters such as pK_a, proton NMR shift, and linear free energy of substituted compounds have been reported to correlate with Hammett constants [3-5]. However, despite successful applications of Hammett constants [6-8], these are not very successful for substituents that were not common [8] or substituents that cause a shift in the position of transition state [5]. To beat this challenge, researchers have introduced new parameters to modify Hammett constants [9,10]. Moreover, quantum chemical methods like electrostatic and ionization potentials [11-12], substituted effect stabilization energy (SESE) [2,13], charge substituent active region (cSAR) [13,14]. Aromaticity indices such as harmonic oscillator model of aromaticity (HOMA) [15] and nucleus independent chemical shifts (NICS) [16], are also used to describe substituent effect in π-conjugated systems especially when they show strong correlations with Hammett constants.

Resonance stabilization has been found to be significantly enhanced by the simultaneous presence of both electron-donating and accepting groups, especially at *para* positions [17,18]. Theoretical studies of substituent effect are shown to be promising for practical applications like in organic dyes and photochromic compounds. Modifying π-spacer of organic dyes by electron-withdrawing groups resulted in the expansion of their absorption range and achieving high performance dye-sensitized solar cell devices [19]. Fluorine substituent exhibited a strong acceleration of the rate of *cis-trans* isomerization of *ortho*-fluoroazobenzene compounds and they also affected the conjugate system of *E* isomer [20]. This lead to an increase in light conversion rate in these photoswitches.

The internal rotational barriers can be linked to conjugation in substituted aromatic systems only in few cases. In some studies, the presence of π-electron acceptors at *para*-position in phenol has been found to increase the rotational barrier due to enhancement of electronic delocalization [21]. The increase in rotational barrier relates to the strength of conjugation in substituted nitrotoluenes, nitrophenols, and nitroanilines, especially in *para*-positions [22]. The nitro group in these compounds is coplanar with the phenyl ring due to conjugation and resonance effects. The barrier to internal rotation increased with the strength of electron-donating substituents in *para*-substituted acetophenones where these substituents led to an increase in the double bond character of the phenyl-acetyl bond [23].

**Corresponding author: Ali Hussain Yateem*
Email address: alihali222@gmail.com
DOI: http://dx.doi.org/10.13171/mjc02004161378ahy

Received March 5, 2020
Accepted March 24, 2020
Published April 16, 2020

A similar conclusion has been reached with *para*-substituted benzaldehydes and p-methoxy-acylbenzenes [24]. The strength of electron-donating and accepting groups based on quantum mechanical methods have been established mostly with some common substituents as shown from the above examples. The main exception is the classification of substituents from very strong to weak electron-donating/withdrawing groups based on molecular electrostatic potential (MESP) analysis [11]. The MESP analysis has also been successful in the study of electron donor-acceptor non-covalent complexes [25,26]. Hence, with the exception of electrostatic potential studies, there is no quantum mechanical method that could quantify the substituent effect with a large number of substituents. Therefore, it is strongly desired to quantify the effects of a large variety of substituents by correlating them with many empirical and computational parameters. These parameters are mandatory for measuring the extent of π-conjugation, which is the underlying reason for resonance stabilization of *para*-substituted conjugated systems.

Spurred on by the importance of correlating a large number of substituents with the stability profile of conjugated systems, the internal rotational barrier was adopted as a quantum mechanical approach to quantify the electron-withdrawing substituents effects in 84 *para*-substituted anilines. The rotational barrier was correlated with empirical Hammett σ_p and pK_a constants, as well with geometric, atomic, molecular, and spectroscopic properties that are affected by electron-withdrawing groups. The substituents are classified between strongly to very weakly electron-withdrawing groups based on RB and their correlation with geometric, atomic, spectroscopic, and molecular properties.

2. Method

The internal rotation potential energy curves were obtained by performing geometry optimization calculations at a set of HNCC dihedral angles ranging from 0 to 130° with an increment of 10°. Close to maximum state the increment was decreased to 1° and then to 0.1°. The minimum equilibrium states were optimized separately.

The internal rotational barrier RB around the C–N bond in aniline was considered between the minimum equilibrium state at a dihedral angle θ between 14.71° and 16.42° and the maximum state at a dihedral θ between 120.23° and 122.60°. Except for the dihedral angle θ, all the independent structural parameters were optimized. The symbol φ represents the out-of-plane angle between the NH_2 plane and the plane formed between the benzene carbons and the nitrogen atom. The minimum ionization potential I(r) was calculated only if it was on lone pair of the amino nitrogen in both minimum and maximum states. The ionization potential is defined by eq. (1)

$$I(\mathrm{r}) = \sum_i \rho_i(\mathrm{r})|\epsilon_i| / \rho(\mathrm{r}) \quad (1)$$

Where ρ_i(r) is the orbital electron density, $|\epsilon_i|$ is absolute orbital energy, and ρ(r) is the total electron density. The maximum electrostatic potential was also calculated only if it was on amino hydrogens of both minimum and maximum states. The minimum ionization and maximum electrostatic potentials were evaluated from QSAR model. The stabilization energy was calculated using the relationship [2,13], eq. (2),

$$\textbf{Stabilization energy} = E\textbf{(benzene–X)} + E\textbf{(aniline)} - E\textbf{(aniline–X)} - E\textbf{(benzene)} \quad (2)$$

Where X is the electron-withdrawing substituent, the large value of stabilization energy means higher stabilization energy due to the substituent effect.

Energies of the minimum and maximum states were corrected for zero-point energies from the measurement of IR vibrational frequencies except in calculation of stabilization energy since it is expected, and tested for selected molecules, that they almost cancel out in the above equation. The character of structure of the minimum and maximum states was confirmed by vibrational frequency analysis. One imaginary vibrational frequency was obtained for maximum states and none for minimum states. The experimental pK_a values and Hammett σ_p constants were obtained according to the methods reported in literature [27-29].

The approach here is to plot changes in structural, atomic, and molecular properties between the minimum and maximum states against the rotational barrier. The difference between these two states resulted in slightly better values of correlation coefficient R^2 in comparison to values of only minimum states, except in the case of NH_2 stretching frequencies where RB was plotted versus the symmetric and asymmetric stretching frequencies of the minimum states. Ionization and electrostatic potentials were taken as the difference between the two states. All computations were carried out at the density functional ωB97X-D level with 6-31G** basis set using Spartan'14 (v. 1.1.4) [30]. The default grid for ωB97X-D method is 75,302. Its gradient termination criteria is 0.007, and its displacement is 0.0014. Substituents considered here are all neutral, and they are ranged from weakly to strongly electron-withdrawing substituents owing to their positive σ_p values. The conformer with the lowest energy was chosen in case there is more than one conformer per molecule after performing conformers distribution analysis. The cationic species $N(CH_3)_3^+$, NH_3^+, and N_2^+ have also been studied but not included in plots. This is because ionization and

electrostatic potentials cannot be located for ionic species in Spartan. The pK_a values for $N(CH_3)_3^+$ and NH_3^+ are unreasonably higher than expected, while N_2^+ is significantly an outlier in all plots.

3. Results and Discussion

3.1. Substituent effect on parameters of para-substituted anilines

Tables 1 and 2 show values of HNCC dihedral angle θ, C–NH_2 bond length R(C–NH_2), H-N-H angle A, out-of-plane angle φ, natural charge on amino nitrogen Q_n, minimum ionization potential IP, and maximum electrostatic potential Es_{max} for minimum and maximum states of 84 *para*-substituted anilines respectively. The available experimental geometrical values are written in parenthesis in Table 1. Also, the calculated N–H distance of amino group in aniline (1.009 Å) is in good agreement with the reported experimental values (0.999–1.026 Å) [39-41]. Therefore, the calculated values either fall within the experimental limits or are reasonably close to them. The calculated ionization potential is around 3 eV higher than experimental values of aniline and few available para-substituted anilines (7.70–8.64 eV) [45]. However, the experimental IP values were found to increase with the increasing power of electron-donating substituents which is similar to the trend in calculated IP here.

C–NH_2 bond distances for all *para*-substituted anilines are smaller or equal to that of aniline (1.394 Å) except for NHCN and F. The C–NH_2 bond for C(CN)=$C(CN)_2$ substituent is 1.365 Å which is the shortest compared to that of aniline. The shorter length of this single bond indicates the increase of its double bond (π component) character. The C–NH_2 bond distance in maximum states are very close to each other and larger than those in minimum states (Table 2) due to the lack of conjugation. The H–N–H angles in minimum states of *para*-substituted anilines are larger than that for aniline. In contrast, the out-of-plane angles φ are smaller except a few exceptions listed at the bottom of Table 1. The increase in H–N–H angle and the decrease of out-of-plane angles in minimum states compared to maximum states are indicative of changing the geometry of NH_2 group from pyramidal to planar. The H–N–H and out-of-plane angles φ in maximum states remained almost unaffected by substituents due to lack of conjugation in maximum states. Thus, NH_2 group in maximum states adopts a typical pyramidal geometry. The decrease in the negative natural charge on amino nitrogen in minimum states (Table 1) suggests a shift of electronic density from nitrogen. The values of natural charge on amino nitrogen in maximum states are almost constant and more negative than those in minimum states.

Table 3 shows that the values of rotational barrier RB and the difference in C–NH_2 bond length, H–N–H bond angle, out-of-plane angle φ, natural charge on amino nitrogen, minimum ionization potential, and maximum electrostatic potential, fall between the minimum and maximum states of *para*-substituted anilines. The substituents are arranged in order of decreasing rotational barrier between the two states. Table 4 shows the empirical pK_a values, symmetric and asymmetric NH_2 stretching frequencies for the minimum states, empirical σ_p values, and the stabilization energy for the minimum states. Plots of parameters in Table 3 versus rotational barriers have been presented in Fig. 1. An observation of Fig. 1a reveals that change in C–NH_2 bond is strongly correlated with RB and, referring to Tables 1 and 2, this correlation is mainly due to changes in minimum states. Bond order was calculated and found to increase, from 1.24 to 1.33, with the increasing power of electron-withdrawing substituents in the minimum states. The bond order remains constant at 1.16 for all substituents in maximum states. The shortening of C–NH_2 bong length and increase of bond order with increasing RB implies that there is an increase in double bond character with increasing RB. It is worth mentioning here that as RB increases, the C–NH_2 bond length becomes closer and even shorter than that of formamide (1.376 Å) which is almost planar [39]. The strong correlation between the changes in H–N–H and out-of-plane angles shown, respectively, in Figs 1b and 1c demonstrates that amino group becomes more open and planar with increasing rotational barrier. The sum of three angles around amino nitrogen atom in minimum state with C(CN)=$C(CN)_2$ substituent, which has the highest RB, is only 5.62° less than the completely planar geometrical structure. The corresponding sum in aniline differs by 18.41° from the planar structure. The increase in flattening of the pyramidal NH_2 with the increasing power of electron-withdrawing substituents has been verified experimentally for many *para*-substituted anilines [33,46,47]. The increase in double-bond character and the opening of the H–N–H angle with RB indicate that the lone pair on amino nitrogen involves more in π-conjugation as RB increases.

It can be seen from Fig. 1d that change in natural charge on the amino nitrogen atom is correlated well with RB. This is attributed to the prominent decrease in a negative value of natural charge in minimum states, as shown in Tables 1 and 2. The decrease in negative value of natural charge with the increase in RB can be attributed to the involvement of lone pair on amino nitrogen in bonding with the adjacent carbon atom of the benzene ring. Natural charges have been shown to be superior to other forms of charges in the systems like the one under study here [3,4,39].

It is found that the lowest ionization potential in most of the compounds studied here is associated with the lone pair of amino nitrogen. This potential is expected to increase with the involvement of the lone pair in conjugation.

Table 1. Calculated geometrical, atomic, and molecular parameters for minimum (equilibrium) state of *para*-substituted anilines. Experimental values are in parenthesis.

Substituent	θ (deg)	R(C-NH_2) (Å)	A(H-N-H) (deg)	φ (deg)	Q_n(N) (e)	IP (eV)	Es_{max} (kcal/mol)
$C(CN)=C(CN)_2$	14.71	1.365	116.02	23.03	-0.836	11.97	65.92
N=NCN	15.65	1.368	115.68	25.00	-0.839		62.88
$SO_2C(CF_3)_3$	17.89	1.371	115.12	28.00	-0.845	11.66	61.36
PF_4	17.71	1.371	115.10	28.26	-0.846	11.47	58.51
SO_2CN	16.84	1.369	115.36	26.49	-0.843	11.78	63.79
BCl_2	18.45	1.373	114.87	29.49	-0.846	11.29	56.29
COCl	18.50	1.373	114.85	29.44	-0.846	11.41	58.32
NO	18.41	1.373	114.77	29.76	-0.845		57.60
SO_2CF_3	17.70	1.372	115.05	28.28	-0.846	11.57	60.64
SO_2Cl	18.08	1.372	114.95	28.65	-0.846	11.64	61.68
N(O)=NCN	18.89	1.372	114.84	29.21	-0.844	11.68	62.43
$COCF_3$	18.82	1.374	114.72	30.12	-0.847	11.36	57.48
$C(NO_2)_3$	18.32	1.372	114.80	29.53	-0.846	11.59	61.18
SO_2F	18.65	1.373	114.80	29.43	-0.847	11.55	60.75
$PSCl_2$	18.38	1.373	114.75	29.73	-0.847		59.58
$P(CN)_2$	19.05	1.374	114.64	30.22	-0.848		59.86
SO_2CHF_2	18.72	1.374	114.78	29.64	-0.848	11.48	59.87
$N=NCF_3$	18.98	1.375	114.58	30.63	-0.847	11.32	57.06
COF	20.08	1.376	114.25	32.12	-0.849	11.24	56.21
$POCl_2$	19.27	1.374	114.62	30.33	-0.848	11.45	59.41
POF_2	19.63	1.375	114.49	30.95	-0.849	11.37	58.43
NO_2	19.42	1.375 (1.37[a],1.371[b])	114.47 (113.6[c])	31.01	-0.848	11.39	58.60
SF_3	19.77	1.375	114.44	31.29	-0.849	11.33	56.88
SCl	20.40	1.377	114.12	32.62	-0.850		55.89
$SiCl_3$	20.34	1.378	114.08	32.75	-0.852	11.22	55.75
CHO	20.79	1.379	113.89	33.62	-0.852	11.07	53.85
PCl_2	20.65	1.377	114.11	32.63	-0.851		56.22
$SiBr_3$	20.65	1.378	113.93	33.41	-0.852	11.18	55.22
$GeCl_3$	20.29	1.377	114.09	32.63	-0.852	11.28	57.23
BF_2	21.46	1.381	113.69	34.56	-0.854	10.97	51.78
$P(CF_3)_2$	20.97	1.378	113.94	33.41	-0.852		54.99
COOH	21.76	1.381 (1.381[d])	113.61 (114[e])	34.86	-0.855	10.94	
SiF_3	21.25	1.380	113.70	34.36	-0.854	11.11	54.01
CN	21.01	1.379 (1.36[f])	113.84	33.67	-0.853	11.21	56.54
PF_2	21.74	1.381	113.59	34.86	-0.854		53.22
SO_2CH_3	20.63	1.379	114.08	32.77	-0.853	11.20	56.00
$COCH_3$	22.20	1.382	113.45	35.44	-0.855	10.91	51.63
SF_5	21.28	1.380	113.69	34.29	-0.854	11.19	55.96
SO_2NH_2	21.59	1.381	113.69	34.38	-0.855	11.07	
5-tetrazolyl	21.90	1.382	113.42	35.31	-0.855		
$SiCl_2CH_3$	21.81	1.382	113.47	35.28	-0.856	10.97	52.61
$CO_2C_2H_5$	22.22	1.383	113.37	35.85	-0.856	10.83	50.23
CO_2CH_3	22.51	1.383	113.32	35.99	-0.856	10.84	50.30
$PO(OH)_2$	22.02	1.382	113.51	35.19	-0.856	10.90	
COC_2H_5	22.38	1.382	113.39	35.66	-0.855	10.90	51.36

Table 1 shows that there is a slight general increase in ionization potential with the increasing power of electron-withdrawing groups in the minimum state but the correlation with the difference in this potential between the minimum and maximum states are clearly shown in Fig. 1e. The local surface ionization energy minima on lone pair of amino nitrogen has been reported to correlate with Hammett σ_p^0 [48] constant and with pK_a [3] in some *para*-substituted anilines.

Table 1. (*continued*)

Substituent	θ (deg)	R(C-NH$_2$) (Å)	A(H-N-H) (deg)	φ (deg)	Q_n(N) (e)	IP (eV)	Es_{max} (kcal/mol)
SCN	21.09	1.380	113.77	33.90	-0.854		55.93
C≡CCF$_3$	21.90	1.382	113.50	35.07	-0.855	11.08	54.31
SeCN	21.11	1.380	113.78	33.92	-0.854		55.46
SCF$_3$	22.15	1.383	113.36	35.64	-0.857		52.76
SiF$_2$CH$_3$	22.54	1.384	113.19	36.45	-0.858	10.83	50.62
SCHF$_2$	23.16	1.385	113.01	36.92	-0.859		51.71
CF$_3$	22.81	1.385	113.02	36.91	-0.858	10.92	51.77
CH(CN)$_2$	22.38	1.383	113.28	35.84	-0.857	11.11	
CH=NOCH$_3$	23.27	1.386	112.86	37.66	-0.859	10.71	48.45
CHBr$_2$	22.50	1.385	113.06	36.75	-0.858	10.89	51.80
COC$_6$H$_5$	22.20	1.382	113.52	35.20	-0.855	10.91	51.40
CHCl$_2$	22.77	1.385	112.96	37.09	-0.859	10.88	51.53
C$_6$F$_5$	23.49	1.387	112.75	37.95	-0.860	10.80	50.18
B(OH)$_2$	23.50	1.388	112.64	38.52	-0.861	10.60	
SiH$_3$	23.75	1.388	112.58	38.65	-0.861	10.66	47.64
CHF$_2$	23.36	1.387	112.71	38.07	-0.861	10.77	49.59
CCH	23.90	1.388	112.58	38.57	-0.861	10.61	48.38
CH$_2$Cl	24.50	1.389	112.33	39.38	-0.862	10.69	48.23
CH$_2$Br	24.48	1.389	112.41	39.11	-0.861		48.49
SH	23.99	1.388	112.50	38.78	-0.862		48.59
GeH$_3$	24.33	1.390	112.30	39.63	-0.863	10.58	46.68
Si(CH$_3$)$_2$C$_6$H$_5$	24.72	1.390	112.30	39.72	-0.864	10.49	44.86
Si(C$_2$H$_5$)$_3$	24.63	1.391	112.22	39.92	-0.864	10.49	44.91
SeCH=CH$_2$	23.53	1.388	112.64	38.36	-0.861		48.88
P(C$_6$H$_5$)$_2$	24.26	1.389	112.56	38.77	-0.862		47.19
I	24.25	1.389 (1.43[g])	112.38	39.16	-0.862		49.78
SCH=CH2	23.80	1.389	112.43	39.02	-0.862		48.65
2-furyl	24.50	1.391	112.13	40.16	-0.864	10.52	45.97
Br	24.55	1.390 (1.401[h])	112.21	39.67	-0.863	10.73	49.42
CH$_2$CN	24.11	1.391	112.13	39.97	-0.864	10.67	48.96
Cl	24.79	1.391 (1.381[i],1.386[j])	112.08	40.09	-0.864	10.70	49.06
CH$_2$OH	25.31	1.394	111.78	41.30	-0.866	10.45	
H	25.42	1.394 (1.402[k],1.407[l])	111.77 (111.15[m],111.8[n], 111.7[o])	41.33 (38-46[p])	-0.867	10.39	43.78
CH$_2$COCH$_3$	25.03	1.392	112.02	40.45	-0.865	10.55	46.75
N=C=O	24.63	1.391	112.06	40.11	-0.864	10.69	49.32
CH$_2$F	25.08	1.393	111.90	40.81	-0.865	10.49	45.79
N$_3$	25.28	1.393	111.84	40.87	-0.865	10.63	48.42
NHCN	25.67	1.396	111.40	42.19	-0.868	10.58	
F	26.42	1.397	111.23 (111.87[q])	42.73 (42.73[r])	-0.869	10.46	45.97

[a]Ref. 31, [b]Ref. 32, [c]Ref. 33, [d]Ref. 34, [e]Ref. 34, [f]Ref. 36, [g]Ref. 33, [h,i]Ref. 37, [j]Ref. 38, [k]Ref. 39, [l]Ref. 40, [m]Ref. 41, [n,o]Ref. 33, [p]Ref. 42, [q]Ref. 43, [r]Ref. 44

Table 2. Calculated geometrical, atomic, and molecular parameters for maximum state of *para*-substituted anilines.

Substituent	θ (deg)	***R*(C-NH$_2$)** (Å)	***A*(H-N-H)** (deg)	φ (deg)	**Q_n(N)** (e)	***IP*** (eV)	***Es*$_{max}$** (kcal/mol)
C(CN)=C(CN)$_2$	120.6	1.432	106.72	54.44	-0.929	10.69	50.02
N=NCN	121.1	1.433	106.53	54.85	-0.930		47.73
SO$_2$C(CF$_3$)$_3$	121.2	1.433	106.69	54.67	-0.929	10.61	48.19
PF$_4$	120.7	1.434	106.30	55.34	-0.929	10.47	45.64
SO$_2$CN	121.0	1.432	106.79	54.39	-0.929	10.72	50.43
BCl$_2$	121.6	1.435	106.34	55.35	-0.929	10.31	43.04
COCl	121.5	1.434	106.55	54.90	-0.929	10.44	45.54
NO	121.3	1.435	106.57	54.86	-0.930		44.51
SO$_2$CF$_3$	121.2	1.433	106.69	54.58	-0.929	10.58	48.20
SO$_2$Cl	121.1	1.433	106.78	54.45	-0.929	10.62	48.76
N(O)=NCN	122.09	1.432	106.86	54.21	-0.928	10.66	49.48
COCF$_3$	121.4	1.434	106.40	55.12	-0.929	10.39	44.71
C(NO$_2$)$_3$	121.3	1.432	106.74	54.51	-0.928	10.64	48.72
SO$_2$F	121.3	1.433	106.62	54.71	-0.929	10.61	48.49
PSCl$_2$	121.2	1.433	106.66	54.68	-0.929		46.73
P(CN)$_2$	121.0	1.433	106.77	54.46	-0.929		47.57
SO$_2$CHF$_2$	121.0	1.434	106.53	54.80	-0.929	10.56	47.54
N=NCF$_3$	121.7	1.435	106.47	54.98	-0.929	10.36	44.15
COF	120.8	1.435	106.40	55.13	-0.929	10.37	44.42
POCl$_2$	121.0	1.434	106.68	54.64	-0.930	10.53	46.68
POF$_2$	121.23	1.434	106.58	54.86	-0.929	10.49	46.18
NO$_2$	121.4	1.434	106.66	54.65	-0.929	10.48	46.39
SF$_3$	121.47	1.434	106.61	54.84	-0.929	10.41	45.05
SCl	121.4	1.435	106.46	55.11	-0.929		43.86
SiCl$_3$	121.3	1.435	106.58	54.86	-0.929	10.35	44.03
CHO	121.4	1.436	106.51	54.96	-0.929	10.24	42.27
PCl$_2$	121.2	1.434	106.56	54.87	-0.929		43.92
SiBr$_3$	121.4	1.435	106.46	55.03	-0.929	10.32	43.46
GeCl$_3$	121.2	1.434	106.63	54.69	-0.929	10.44	45.52
BF$_2$	121.3	1.436	106.27	55.44	-0.929	10.16	40.71
P(CF$_3$)$_2$	121.37	1.435	106.58	54.87	-0.929		43.66
COOH	121.6	1.436	106.39	55.20	-0.929	10.15	
SiF$_3$	121.4	1.435	106.53	54.95	-0.929	10.32	43.05
CN	121.9	1.434	106.36	55.03	-0.928	10.42	45.31
PF$_2$	121.54	1.436	106.57	54.88	-0.929		42.23
SO$_2$CH$_3$	121.8	1.435	106.63	54.71	-0.929	10.38	44.97
COCH$_3$	121.6	1.436	106.43	55.08	-0.929	10.14	40.67
SF$_5$	121.48	1.434	106.72	54.58	-0.928	10.43	45.06
SO$_2$NH$_2$	121.4	1.435	106.64	54.75	-0.929	10.29	
5-tetrazolyl	121.5	1.435	106.71	54.46	-0.928		
SiCl$_2$CH$_3$	121.5	1.436	106.37	55.23	-0.929	10.22	41.39
CO$_2$C$_2$H$_5$	121.5	1.436	106.40	55.22	-0.929	10.09	39.27
CO$_2$CH$_3$	121.4	1.437	106.32	55.38	-0.929	10.10	39.29
PO(OH)$_2$	121.32	1.436	106.46	55.14	-0.929	10.18	
COC$_2$H$_5$	121.98	1.436	106.19	55.54	-0.929	10.15	39.95
SCN	121.9	1.435	106.60	54.71	-0.928		45.06
C≡CCF$_3$	120.9	1.435	106.45	54.94	-0.928	10.31	43.11

Table 2. (*continued*)

Substituent	θ (deg)	R(C-NH_2) (Å)	A(H-N-H) (deg)	φ (deg)	Q_n(N) (e)	IP (eV)	Es_{max} (kcal/mol)
SeCN	121.18	1.435	106.50	54.89	-0.928		44.67
SCF_3	121.25	1.435	106.56	54.89	-0.929		42.24
SiF_2CH_3	121.1	1.437	106.39	55.23	-0.929	10.12	40.03
$SCHF_2$	122.16	1.436	106.45	54.98	-0.928		41.55
CF_3	121.3	1.436	106.54	54.86	-0.928	10.24	41.74
$CH(CN)_2$	121.78	1.435	106.44	54.89	-0.928	10.43	
$CH{=}NOCH_3$	121.77	1.437	106.33	55.25	-0.928	9.99	37.88
$CHBr_2$	121.4	1.436	106.57	54.83	-0.928	10.17	41.18
COC_6H_5	122.0	1.436	106.27	55.36	-0.929	10.12	39.88
$CHCl_2$	120.87	1.436	106.31	55.21	-0.928	10.21	41.11
C_6F_5	121.5	1.436	106.45	55.03	-0.928	10.13	40.08
$B(OH)_2$	121.8	1.438	106.31	55.45	-0.929	9.95	
SiH_3	121.7	1.437	106.42	55.17	-0.929	10.01	37.98
CHF_2	121.36	1.436	106.47	55.00	-0.928	10.15	39.98
CCH	121.4	1.437	106.47	54.97	-0.928	10.04	38.47
CH_2Cl	122.3	1.437	106.40	55.06	-0.928	10.06	39.14
CH_2Br	121.0	1.437	106.47	55.01	-0.928		39.03
SH	121.4	1.437	106.44	55.02	-0.928		39.40
GeH_3	121.4	1.437	106.41	55.15	-0.928	9.97	37.37
$Si(CH_3)_2C_6H_5$	122.02	1.438	106.19	55.56	-0.929	9.86	35.24
$Si(C_2H_5)_3$	121.73	1.438	106.19	55.53	-0.928	9.88	35.58
$SeCH{=}CH_2$	121.23	1.437	106.20	55.30	-0.927		38.31
$P(C_6H_5)_2$	122.6	1.438	106.13	55.59	-0.928		37.04
I	122.1	1.436	106.43	54.93	-0.927		40.08
SCH=CH2	121.0	1.437	106.60	54.70	-0.928		38.11
2-furyl	121.7	1.437	106.40	55.05	-0.928	9.90	36.28
Br	121.9	1.436	106.41	54.92	-0.927	10.15	40.31
CH_2CN	121.1	1.437	106.44	54.98	-0.928	10.10	39.45
Cl	121.9	1.436	106.40	54.90	-0.927	10.13	39.98
CH_2OH	121.01	1.438	106.11	55.41	-0.927	9.92	
H	121.7	1.438	106.46	55.06	-0.928	9.86	35.49
CH_2COCH_3	122.2	1.437	106.32	55.17	-0.928	9.99	37.55
N=C=O	120.23	1.436	106.25	55.01	-0.927	10.13	40.07
CH_2F	121.28	1.437	106.52	54.80	-0.928	9.92	36.70
N_3	121.18	1.436	106.74	54.29	-0.928	10.08	39.21
NHCN	121.17	1.436	106.56	54.43	-0.926	10.10	
F	121.12	1.437	106.43	54.73	-0.927	10.02	37.99

Table 3. Rotational barrier and differences of geometrical, atomic, and molecular parameters between minimum (Table 1) and maximum states (Table 2) of *para*-substituted anilines.

Substituent	**RB** (kcal/mol)	**Δ*R*(C-NH$_2$)** (Å)	**Δ*A*(H-N-H)** (deg)	**Δ*φ*** (deg)	**ΔQ_n(N)** (e)	**Δ*IP*** (eV)	**ΔEs_{max}** (kcal/mol)
C(CN)=C(CN)$_2$	8.99	-0.067	9.30	-31.41	0.093	1.28	15.90
N=NCN	8.75	-0.065	9.15	-29.85	0.091		15.15
SO$_2$C(CF$_3$)$_3$	8.75	-0.062	8.43	-26.67	0.084	1.05	13.17
PF$_4$	8.57	-0.063	8.80	-27.08	0.083	1.00	12.87
SO$_2$CN	8.46	-0.063	8.57	-27.90	0.086	1.06	13.36
BCl$_2$	8.22	-0.062	8.53	-25.86	0.083	0.98	14.94
COCl	8.08	-0.061	8.30	-25.46	0.083	0.97	13.24
NO	8.07	-0.062	8.20	-25.10	0.085		12.77
SO$_2$CF$_3$	8.05	-0.061	8.36	-26.30	0.083	0.99	13.08
SO$_2$Cl	8.04	-0.061	8.17	-25.80	0.083	1.02	12.44
N(O)=NCN	8.00	-0.060	7.98	-25.00	0.084	1.02	12.92
COCF$_3$	8.00	-0.060	8.32	-25.00	0.082	0.97	12.95
C(NO$_2$)$_3$	7.93	-0.060	8.06	-24.98	0.082	0.95	12.77
SO$_2$F	7.91	-0.060	8.18	-25.28	0.082	0.94	12.46
PSCl$_2$	7.83	-0.060	8.09	-24.95	0.082		12.26
P(CN)$_2$	7.81	-0.059	7.87	-24.24	0.081		12.85
SO$_2$CHF$_2$	7.75	-0.060	8.25	-25.16	0.081	0.92	12.29
N=NCF$_3$	7.72	-0.060	8.11	-24.35	0.082	0.96	12.33
COF	7.71	-0.059	7.85	-23.01	0.080	0.87	12.91
POCl$_2$	7.71	-0.060	7.94	-24.31	0.082	0.92	11.79
POF$_2$	7.66	-0.059	7.91	-23.91	0.080	0.88	12.74
NO$_2$	7.65	-0.059	7.81	-23.64	0.081	0.91	12.25
SF$_3$	7.58	-0.059	7.83	-23.55	0.080	0.92	12.20
SCl	7.44	-0.058	7.66	-22.49	0.079		11.83
SiCl$_3$	7.32	-0.057	7.50	-22.11	0.077	0.87	12.03
CHO	7.29	-0.057	7.38	-21.34	0.077	0.83	10.75
PCl$_2$	7.28	-0.057	7.55	-22.24	0.078		11.71
SiBr$_3$	7.26	-0.057	7.47	-21.62	0.077	0.86	11.58
GeCl$_3$	7.22	-0.057	7.46	-22.06	0.077	0.84	12.30
BF$_2$	7.22	-0.055	7.42	-20.88	0.075	0.81	11.77
P(CF$_3$)$_2$	7.18	-0.057	7.36	-21.46	0.077		11.71
COOH	7.08	-0.055	7.22	-20.34	0.074	0.79	11.07
SiF$_3$	7.08	-0.055	7.17	-20.59	0.075	0.79	11.33
CN	7.03	-0.055	7.48	-21.36	0.075	0.79	
PF$_2$	6.99	-0.055	7.02	-20.02	0.075		10.96
SO$_2$CH$_3$	6.97	-0.056	7.45	-21.94	0.076	0.82	11.22
COCH$_3$	6.94	-0.054	7.02	-19.64	0.074	0.77	10.98
SF$_5$	6.91	-0.054	6.97	-20.29	0.074	0.76	11.03
SO$_2$NH$_2$	6.81	-0.054	7.05	-20.37	0.074	0.78	10.95
5-tetrazolyl	6.79	-0.053	6.71	-19.15	0.073		10.90
SiCl$_2$CH$_3$	6.78	-0.054	7.10	-19.95	0.073	0.75	
CO$_2$C$_2$H$_5$	6.78	-0.053	6.97	-19.37	0.073	0.74	
CO$_2$CH$_3$	6.76	-0.054	7.00	-19.39	0.073	0.74	11.22
PO(OH)$_2$	6.73	-0.054	7.05	-19.95	0.073	0.72	10.96
COC$_2$H$_5$	6.72	-0.054	7.20	-19.88	0.074	0.75	11.01
SCN	6.71	-0.055	7.17	-20.81	0.074		
C≡CCF$_3$	6.70	-0.053	7.05	-19.87	0.073	0.77	11.41

SeCN	6.69	-0.055	7.28	-20.97	0.074		10.87

Table 3. (*continued*)

Substituent	**RB** (kcal/mol)	**Δ*R*(C-NH$_2$)** (Å)	**Δ*A*(H-N-H)** (deg)	**Δ*φ*** (deg)	**ΔQ_n(N)** (e)	**Δ*IP*** (eV)	**ΔEs_{max}** (kcal/mol)
SCF_3	6.49	-0.052	6.80	-19.25	0.072		11.88
SiF_2CH_3	6.39	-0.053	6.80	-18.78	0.071	0.71	11.20
$SCHF_2$	6.36	-0.051	6.56	-18.06	0.069		10.79
CF_3	6.34	-0.051	6.48	-17.95	0.070	0.68	10.09
$CH(CN)_2$	6.29	-0.052	6.84	-19.05	0.071	0.68	10.52
$CH=NOCH_3$	6.28	-0.051	6.53	-17.59	0.069	0.72	10.59
$CHBr_2$	6.27	-0.051	6.49	-18.08	0.070	0.72	10.16
COC_6H_5	6.14	-0.054	7.25	-20.16	0.074	0.79	10.02
$CHCl_2$	6.08	-0.051	6.65	-18.12	0.069	0.67	11.50
C_6F_5	6.06	-0.049	6.30	-17.08	0.068	0.67	
$B(OH)_2$	6.06	-0.050	6.33	-16.93	0.068	0.65	10.57
SiH_3	5.95	-0.049	6.16	-16.52	0.068	0.65	10.62
CHF_2	5.93	-0.049	6.24	-16.93	0.067	0.62	11.52
CCH	5.89	-0.049	6.11	-16.40	0.067	0.57	9.97
CH_2Cl	5.78	-0.048	5.93	-15.68	0.066	0.63	10.43
CH_2Br	5.77	-0.048	5.94	-15.90	0.067		10.10
SH	5.69	-0.049	6.06	-16.24	0.066		
GeH_3	5.64	-0.047	5.89	-15.52	0.065	0.61	9.67
$Si(CH_3)_2C_6H_5$	5.64	-0.048	6.11	-15.84	0.065	0.63	9.77
$Si(C_2H_5)_3$	5.64	-0.047	6.03	-15.61	0.064	0.61	9.61
$SeCH=CH_2$	5.62	-0.049	6.44	-16.94	0.066		10.02
$P(C_6H_5)_2$	5.57	-0.049	6.43	-16.82	0.066		9.62
I	5.52	-0.047	5.95	-15.77	0.065		9.91
SCH=CH2	5.44	-0.048	5.83	-15.68	0.066		9.09
2-furyl	5.40	-0.046	5.73	-14.89	0.064	0.62	9.46
Br	5.32	-0.046	5.80	-15.25	0.064	0.58	10.63
CH_2CN	5.30	-0.046	5.69	-15.01	0.064	0.57	10.77
Cl	5.16	-0.045	5.68	-14.81	0.063	0.57	9.19
CH_2OH	5.13	-0.044	5.67	-14.11	0.061	0.53	9.31
H	5.12	-0.044	5.31	-13.73	0.061	0.53	9.62
CH_2COCH_3	5.11	-0.045	5.70	-14.72	0.063	0.56	9.33
N=C=O	5.02	-0.045	5.81	-14.90	0.063	0.56	10.56
CH_2F	5.01	-0.044	5.38	-13.99	0.063	0.57	10.87
N_3	4.80	-0.043	5.10	-13.42	0.063	0.55	10.15
NHCN	4.43	-0.040	4.84	-12.24	0.058	0.48	9.70
F	4.18	-0.040	4.80	-12.00	0.058	0.44	10.53

Table 4. Rotational barrier, empirical pK_a constants, symmetric and asymmetric NH_2 stretching frequencies, empirical Hammett σ_p constants, and the stabilization energy of *para*-substituted anilines.

Substituent	**RB** (kcal/mol)	**pK_a**	**$n_s(NH_2)$** (cm^{-1})	**$n_a(NH_2)$** (cm^{-1})	**σ_p**	**SE** (kcal/mol)
$C(CN)=C(CN)_2$	8.99		3669	3795	0.98	4.39
N=NCN	8.75		3666	3790	1.03	4.19
$SO_2C(CF_3)_3$	8.75		3660	3783	1.13	3.69
PF_4	8.57		3664	3786	0.8	3.89
SO_2CN	8.46		3667	3790	1.26	3.85
BCl_2	8.22		3660	3782		3.72
COCl	8.08		3661	3782	0.61	3.47
NO	8.07		3657	3778	0.91	3.42
SO_2CF_3	8.05		3657	3781	0.96	3.39
SO_2Cl	8.04		3663	3785	1.11	3.33
N(O)=NCN	8.00		3662	3784	0.89	3.28
$COCF_3$	8.00		3660	3781	0.8	3.39
$C(NO_2)_3$	7.93		3661	3783	0.82	3.37
SO_2F	7.91		3662	3783	0.91	3.24
$PSCl_2$	7.83		3660	3782	0.8	3.20
$P(CN)_2$	7.81		3657	3777	0.9	3.02
SO_2CHF_2	7.75		3656	3778	0.86	2.97
$N=NCF_3$	7.72		3657	3777	0.68	3.01
COF	7.71		3655	3774	0.7	2.96
$POCl_2$	7.71		3656	3776	0.9	3.14
POF_2	7.66		3658	3778	0.89	3.06
NO_2	7.65	1.045	3659	3779	0.778	2.84
SF_3	7.58		3656	3776	0.8	3.05
SCl	7.44		3651	3769	0.48	2.70
$SiCl_3$	7.32		3654	3772	0.56	2.66
CHO	7.29	1.76	3646	3765	0.42	2.49
PCl_2	7.28		3655	3774	0.61	2.61
$SiBr_3$	7.26		3652	3771	0.57	2.58
$GeCl_3$	7.22		3654	3773	0.79	2.55
BF_2	7.22		3648	3766	0.48	2.48
$P(CF_3)_2$	7.18		3648	3766	0.69	2.51
COOH	7.08	2.32	3648	3765	0.45	2.16
SiF_3	7.08		3649	3767	0.69	2.35
CN	7.03	1.74	3652	3770	0.66	2.21
PF_2	6.99		3642	3759	0.59	2.28
SO_2CH_3	6.97	1.48	3654	3773	0.72	2.12
$COCH_3$	6.94	2.19	3645	3762	0.502	2.03
SF_5	6.91		3651	3768	0.68	2.04
SO_2NH_2	6.81	2.02	3651	3768	0.57	1.93
5-tetrazolyl	6.79		3648	3765	0.56	1.78
$SiCl_2CH_3$	6.78		3642	3759	0.39	2.03
$CO_2C_2H_5$	6.78	2.38	3639	3756	0.45	1.93
CO_2CH_3	6.76	2.3	3640	3756	0.45	1.95
$PO(OH)_2$	6.73		3648	3765	0.42	1.93
COC_2H_5	6.72		3640	3757	0.48	2.04
SCN	6.71		3651	3769	0.52	1.89

C≡CCF$_3$	6.70		3648	3765	0.51	1.79
SeCN	6.69		3651	3769	0.66	1.84

Table 4. (*continued*)

Substituent	**RB** (kcal/mol)	**pK_a**	**n_s(NH$_2$)** (cm^{-1})	**n_a(NH$_2$)** (cm^{-1})	**σ_p**	**SE** (kcal/mol)
SCF$_3$	6.49		3649	3765	0.5	1.66
SiF$_2$CH$_3$	6.39		3647	3763	0.23	1.69
SCHF$_2$	6.36		3642	3758	0.37	1.32
CF$_3$	6.34	2.57	3644	3759	0.54	1.44
CH(CN)$_2$	6.29		3645	3761	0.52	1.41
CH=NOCH$_3$	6.28		3641	3756	0.3	1.30
CHBr$_2$	6.27		3639	3755	0.32	1.24
COC$_6$H$_5$	6.14	2.17	3644	3761	0.43	1.91
CHCl$_2$	6.08		3646	3761	0.32	1.24
C$_6$F$_5$	6.06		3641	3755	0.27	1.08
B(OH)$_2$	6.06		3641	3755	0.12	1.30
SiH$_3$	5.95		3638	3752	0.1	1.09
CHF$_2$	5.93		3633	3747	0.32	1.08
CCH	5.89		3639	3753	0.23	0.87
CH$_2$Cl	5.78		3637	3750	0.12	0.79
CH$_2$Br	5.77		3638	3751	0.14	0.83
SH	5.69		3639	3752	0.15	0.84
GeH$_3$	5.64		3637	3749	0.01	0.76
Si(CH$_3$)$_2$C$_6$H$_5$	5.64		3633	3746	0.07	0.82
Si(C$_2$H$_5$)$_3$	5.64		3627	3740		0.69
SeCH=CH$_2$	5.62		3636	3750	0.21	0.45
P(C$_6$H$_5$)$_2$	5.57		3638	3752	0.19	0.87
I	5.52	3.78	3638	3751	0.18	0.43
SCH=CH2	5.44		3637	3750	0.21	0.21
2-furyl	5.40		3633	3745	0.02	0.20
Br	5.32	3.91	3638	3750	0.232	0.16
CH$_2$CN	5.30		3632	3745	0.18	0.36
Cl	5.16	4.15	3637	3749	0.227	-0.04
CH$_2$OH	5.13		3623	3734	0	0.00
H	5.12	4.58	3632	3743	0	0.00
CH$_2$COCH$_3$	5.11		3629	3741		0.06
N=C=O	5.02		3634	3747	0.19	-0.18
CH$_2$F	5.01		3629	3740	0.11	0.03
N$_3$	4.80		3633	3745	0.08	-0.47
NHCN	4.43		3629	3739	0.06	-1.13
F	4.18	4.65	3629	3738	0.062	-1.27

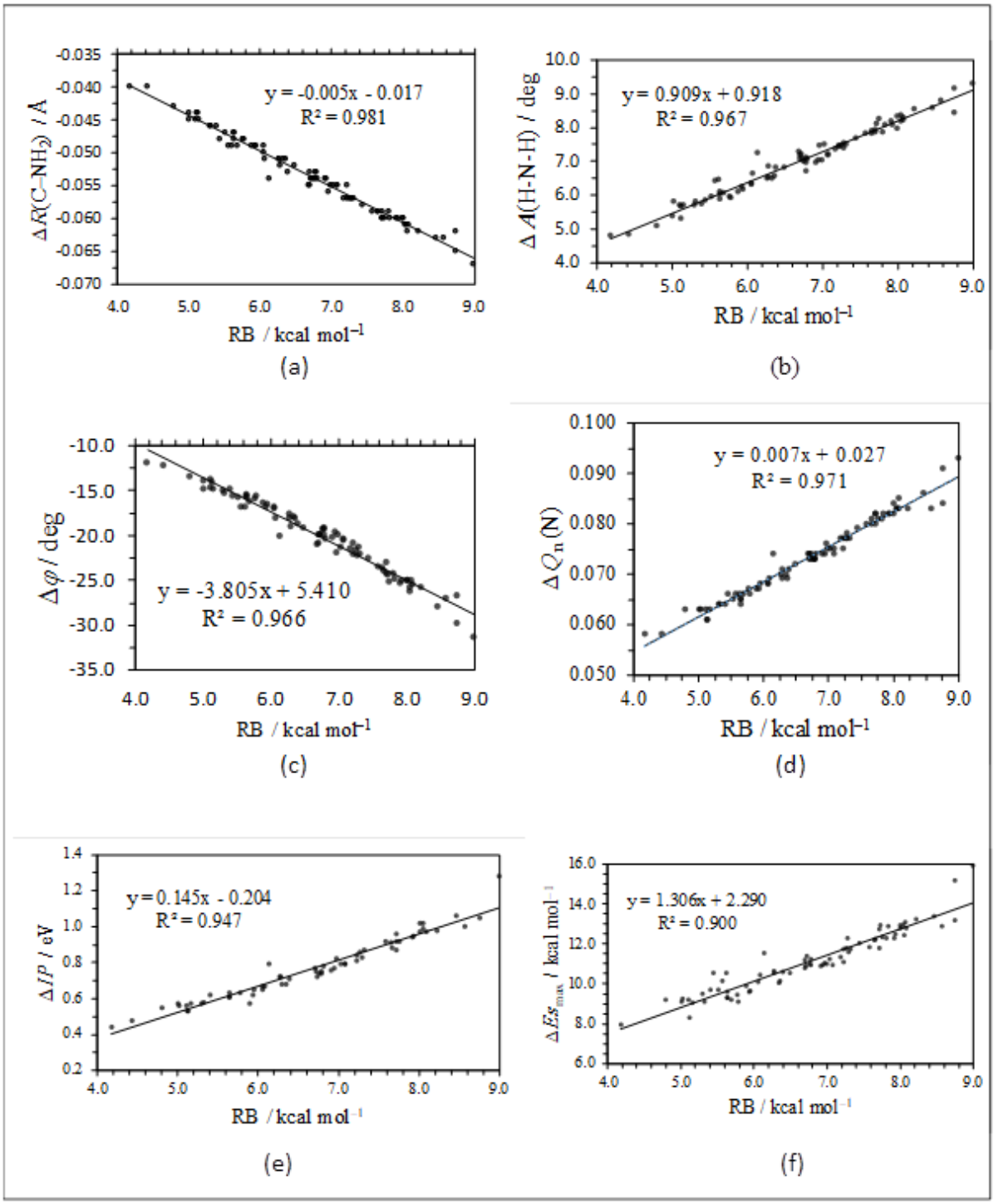

Figure 1. Plots of changes of (a) C-NH_2 bond distance, (b) H-N-H angle, (c) out-of-plane angle, (d) natural charge on amino nitrogen, (e) minimum ionization potential, and (f) maximum electrostatic potential between the minimum and maximum states versus rotational barrier of *para*-substituted anilines

Except for 8 structures, it was found that the maximum (positive) molecular electrostatic potential is in the vicinity of the two amino hydrogens (not a particular hydrogen atom) in *para*-substituted anilines. One can expect that as the electron density is shifted away from these hydrogens, they will have more positive electrostatic potential and that the amino group will be more acidic. Therefore, pK_a values will decrease with the strength of electron-withdrawing groups attached at *para*-position [3,4]. The correlation of changes in electrostatic potential and pK_a values with RB have been presented quantitatively in Figs. 1f and 2a, respectively. The order of substituents in terms of strength of electron-donating follows in general that obtained from molecular electrostatic potential analysis [11].

It was shown experimentally that the force constant, and hence stretching frequency of N–H bond, increases with the increasing power of electron-

withdrawing groups in *para*-substituted anilines. This was attributed to the increasing "*s"* character of the hybrid orbital of the N–H bond relative to π-electron charge density on nitrogen atom [33,47,49]. The experimental symmetric and asymmetric NH_2 stretching vibrations of aniline occur at 3373-3396 cm^{-1} and 3460-3481 cm^{-1}, respectively [33,47,49]. The corresponding experimental values for 10 *para*-substituted anilines fall in the range of 3394-3416 cm^{-1} and 3479-3509 cm^{-1}, respectively [33,49,50]. The calculated stretching frequencies here are 200 cm^{-1} more than the experimental values. However, the trend is the same as that observed experimentally; the symmetric and asymmetric stretching frequencies increase with increasing strength of electron-withdrawing substituents and hence with RB. The RB is shown to correlate well with NH_2 stretching frequencies of the minimum states of *para*-substituted anilines (Fig. 2b). For maximum states of para-substituted anilines, the stretching frequencies were found to change very slightly. Moreover, this change is not related to the strength of electron-withdrawing substituents due to absence of conjugation in the maximum states.

The correlation of empirical Hammett σ_p values with RB has been shown in Fig. 2c. The correlation (R^2 = 0.852) is lower as compared to other parameters, but it is not unexpected considering the reported modifications and corrections to these constants [9,10]. Finally, the stabilization energy is highly correlated to RB as shown in Fig. 2d. The larger stabilization energy corresponds to the role of substituents [13].

3.2 π-conjugation and rotational barrier

It was found that the bond between an atom of X attached to benzene carbon (C–X distance) is shorter in *para*-substituted anilines compared to that in the absence of NH_2 group. Moreover, the difference between these two distances in the minimum states increases with RB, ranging from almost 0 to 0.021 Å. On the other hand, as stated above, the C–NH_2 bond distances in *para*-substituted anilines are shorter than that in aniline, ranging from almost 0 to 0.029 Å. This implies that simultaneous presence of aniline, a typical strong electron-donating group, and electron-withdrawing groups causes more shortening of C–NH_2 and C–X bond distances compared to the presence of any one of them.

The shortening of C–NH_2 bond, the increase in planarity of NH_2 group, the decrease in natural charge on N, and decrease in the basicity of NH_2 group in the presence of electron-withdrawing groups indicates that lone amino pair is conjugated with the pi bond of carbon of benzene ring. The resonance stabilization is extended to substituent X. The decrease in natural charge on amino nitrogen, the increase of minimum ionization and maximum electrostatic potentials, and the increase in NH_2 stretching frequencies with the increasing power of electron-withdrawing substituents further support the electronic delocalization in all the molecules studied here. The fact that these geometric, atomic, and molecular effects correlate strongly with RB, implies that RB is an excellent measure of π-resonance stabilization in *para*-substituted anilines. Moreover, the RB was found to be in good correlation with the empirical constants pK_a and σ_p. A quantitative scale for the ability of electron-withdrawing groups to resonance with aniline can be constructed in terms of RB. As discussed *vide supra*, the π-conjugation system is stabilized by the presence of both NH_2 and electron-withdrawing groups in the para position. Based on this discussion, one can expect scheme 1a to be dominant if RB is more, i.e., the substituent X should be strongly electron-withdrawing. Groups with low RB are presumed to have structures similar to that in scheme 1b which is much similar to aniline. It was found that central C–C bond distances of benzene in *para*-substituted anilines are shorter than the lateral C–C bond distances thus supporting the proposed schemes. Substituents with intermediate RB are expected to fall between these two schemes.

By measuring the natural charge on benzene carbon bonded to substituent X, it is found that this carbon becomes more positive as the atom of X attached to carbon is more electronegative, being largest (+0.393) in case of F substituent followed by O atom in OSO_2CH_3 (+0.225), and then by N atom in NHCN (+0.131). RB in case of OSO_2CH_3 is only 5.33 kcal/mol, and with F and NHCN, the RBs have their lowest values, 4.18 and 4.43 kcal/mol, respectively. On the other hand, with substituents of high RB like NNCN and N(O)=NCN, the natural charge on C atom bonded to N atom in NNCN and N(O)=NCN are only +0.028 and +0.018, respectively. Therefore, the electron-withdrawing inductive effect is expected to have a negligible effect as compared to π-conjugated systems shown here.

This is the first study that quantifies the relation of the electron-withdrawing effect of substituents with RB and correlates the RB barrier to some parameters that are affected by conjugation. It can be considered as a successful alternative quantum mechanical measurement of substituents effects and π conjugation versus the empirical Hammett constants. The opposite atomic, geometrical, and molecular effects were also recorded with several electron-donating substituents in *para*-position to aniline (not shown). A similar study with the same level of

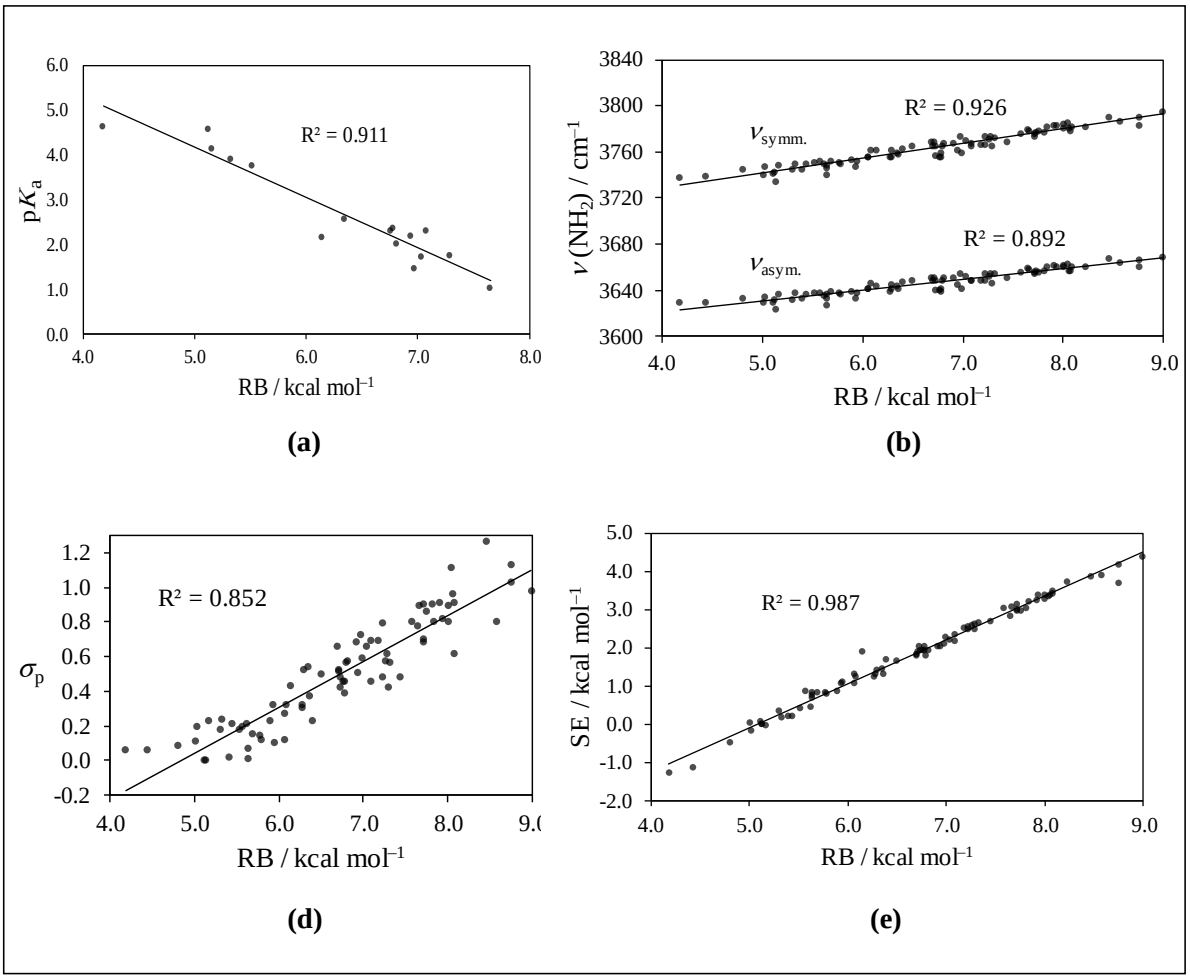

Figure 2. Plots of (a) pK_a constants, (b) symmetric and asymmetric NH_2 stretching frequencies, (c) Hammett σ_p constants, and (d) the stabilization energy versus rotational barrier of *para*-substituted anilines

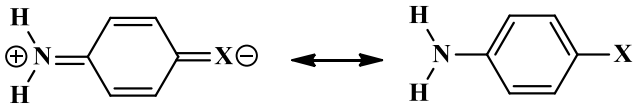

Scheme 1. Two resonance structures of *para*-substituted anilines for which X refers to strong resonance-acceptor substituents (a), or weak electron-withdrawing substituents (b)

The theory showed that RB is a measure of π-conjugation between the donors NH_2 and OCH_3 with few electron-withdrawing groups in disubstituted 1,3-butadienes [51]. Strong correlations were also obtained for several geometrical and spectroscopic parameters vs RB for electron-donating substituents in para-position to benzaldehyde (not published yet). Hence, this study is highly likely to be successfully applied to a large variety of different electron-donating and withdrawing substituents to determine their relative strengths.

4. Conclusion

The ωB97X-D/6-31G** calculations show that the rotational barrier RB between the maximum and minimum states of para-substituted anilines with electron-withdrawing groups is a reliable quantum mechanical measure of π-conjugation in these compounds. The extent of conjugation is verified by several atomic, structural, spectroscopic, and molecular parameters which are shown to be sensitive to substituents and correlate very well with the RB. Moreover, results of the quantum mechanical approach reveal that the RB also correlates well with empirical pK_a and σ_p constants. Hence, based on RB, a scale for the strength of

electron-withdrawing substituents and their ability to resonate with aniline can be established.

References

1- L. P. Hammett, The effect of structure upon the reactions of organic compounds. Benzene derivatives, Journal of the American Chemical Society, **1937**, 59(1), 96-103.
2- T. M. Krygowski, B. T. Stępień, Sigma-and pi-electron delocalization: Focus on substituent effects, Chemical Reviews, **2005**, 105(10), 3482-3512.
3- K. C. Gross, P. G. Seybold, Z. Peralta-Inga, J. S. Murray, P. Politzer, Comparison of quantum chemical parameters and Hammett constants in correlating pKa values of substituted anilines, The Journal of Organic Chemistry, **2001**, 66(21), 6919-6925.
4- K. C. Gross, P. G. Seybold, Substituent effects on the physical properties and pKa of aniline, International Journal of Quantum Chemistry, **2000**, 80(4-5), 1107-1115.
5- T. H. Lowry, K. S. Richardson, Mechanism and theory in organic chemistry (3rd ed.); Harper Collins Publishers: New York, **1987**, pp. 232-244.
6- A. R. Katritzky, R. D. Topsom. Infrared intensities: A guide to intramolecular interactions in conjugated systems, Chemical Reviews, **1977**, 77(5), 639-658.
7- T. M. Krygowski, B. T. Stępień, Sigma-and pi-electron delocalization: Focus on substituent effects. Chemical Reviews, **2005**, 105(10), 3482-3512.
8- P. Ertl, Simple quantum chemical parameters as an alternative to the Hammett sigma constants in QSAR studies, Quantitative Structure-Activity Relationships, **1997**, 16(5), 377-382.
9- C. Hansch, A. Leo, R. W. Taft, A survey of Hammett substituent constants and resonance and field parameters, Chemical Reviews, **1991**, 91(2), 165-195.
10- H. H. Jaffé, A reexamination of the Hammett equation, Chemical Reviews, **1953**, 53(2), 191-261.
11- G. S. Remya, C. H. Suresh, Quantification and classification of substituent effects in organic chemistry: A theoretical molecular electrostatic potential study, Physical Chemistry Chemical Physics, **2016**, 18(30), 20615-20626.
12- P. Politzer, J. S. Murray, F. A. Bulat, Average local ionization energy: a review, Journal of Molecular Modeling, **2010**, 16(11), 1731-1742.
13- H. Szatylowicz, T. Siodla, O. A. Stasyuk, T. M. Krygowski, Towards physical interpretation of substituent effects: the case of meta-and para-substituted anilines, Physical Chemistry Chemical Physics, **2016**, 18(17), 11711-11721.
14- T. M. Krygowski, N. Sadlej-Sosnowska, Towards physical interpretation of Hammett constants: charge transferred between active regions of substituents and a functional group, Structural Chemistry, **2011**, 22(1), 17-22.
15- T. M. Krygowski, Crystallographic studies of inter-and intramolecular interactions reflected in aromatic character of π-electron systems, Journal of chemical information and computer sciences, **1993**, 33(1), 70-78.
16- P. V. Schleyer, M. Manoharan, Z. X. Wang, B. Kiran, H. Jiao, R. Puchta , N. J. van Eikema Hommes, Dissected nucleus-independent chemical shift analysis of π-aromaticity and antiaromaticity, Organic Letters, **2001**, 3(16), 2465-2468.
17- O. Exner, S. Böhm, Conjugation of two functional groups through an unsaturated system, Journal of Physical Organic Chemistry, **2006**, 19(1), 1-9.
18- A. N. Rashid, Basis set effects on the ground and excited state of nitrogen containing organic molecules. p-Nitroaniline as a case study, Journal of Molecular Structure: THEOCHEM, **2004**, 681(1-3), 57-63.
19- L. J. He, J. Chen, F. Q. Bai, R. Jia, J. Wang, H. X. Zhang, Fine-tuning π-spacer for high efficiency performance DSSC: A theoretical exploration with D− π− A based organic dye, Dyes and Pigments, **2017**, 141, 251-261.
20- X. M. Liu, X. Y. Jin, Z. X. Zhang, J. Wang, F. Q. Bai, Theoretical study on the reaction mechanism of the thermal cis–trans isomerization of fluorine-substituted azobenzene derivatives, RSC advances, **2018**, 8(21), 11580-11588.
21- W. Zierkiewicz, D. Michalska, P. Hobza, The barrier to internal rotation and electronic effects in para-halogenophenols: theoretical study, Chemical Physics Letters, **2004**, 386(1-3), 95-100.
22- P. C. Chen and S. C. Chen, Theoretical study of the internal rotational barriers in nitrotoluenes, nitrophenols, and nitroanilines, Computers & Chemistry, **2002**, 26(2), 171-178.
23- A. Haloui and Y. Arfaoui, A DFT study of the conformational behavior of para-substituted acetophenones in vacuum and in various solvents, Journal of Molecular Structure: THEOCHEM, **2010**, 950(1-3), 13-19.
24- T. Drakenberg, J. Sommer, R. Jost, The torsional barrier in aromatic carbonyl compounds, Journal of the Chemical Society, Perkin Transactions 2, **1980,** (2), 363-269.
25- P. V. Bijina, C. H. Suresh, Molecular electrostatic potential analysis of non-covalent complexes, Journal of Chemical Sciences, **2016**, 128(10), 1677-1686.
26- N. Mohan, C. H. Suresh, A molecular electrostatic potential analysis of hydrogen, halogen, and dihydrogen bonds, The Journal of Physical Chemistry A, **2014**, 118(9), 1697-1705.
27- A. Albert, E. P. Serjeant, Ionization Constants of Acids and Bases; Methuen: London, **1962**.

28- D. D. Perrin, Dissociation Constants of Organic Bases in Aqueous Solution; Butterworths: London, **1965**.
29- C. Hansch, A. Leo, R. W. Taft, A survey of Hammett substituent constants and resonance and field parameters, Chemical Reviews, **1991**, 91(2), 165-195.
30- SPARTAN'14. Irvine, CA, USA: Wavefunction, 2014.
31- J. Donohue, K. Trueblood, The crystal structure of p-nitroaniline, Acta Crystallographica, **1956**, 9(11), 960-965.
32- N. I. Sadova, N. P. Penionzhkevich, L. V. Vilkov, Study of the structure of the molecule of para-nitroaniline p−$C_6H_4(NO_2)(NH_2)$ by gaseous electron diffraction, Journal of Structural Chemistry, **1976**, 17(6), 954-956.
33- P. J. Krueger, The vibrational mechanism of the fundamental NH_2 stretching vibrations in anilines, Canadian Journal of Chemistry, **1962**, 40(12), 2300-2316.
34- A. F. Lago, J. Z. Davalos, AN de Brito, A density functional and ab initio investigation of the p-aminobenzoic acid molecule, Chemical Physics Letters, **2007**, 443(4-6), 232-236.
35- T. F. Lai, R. E. Marsh, The crystal structure of p-aminobenzoic acid, Acta Crystallographica, **1967**, 22(6), 885-893.
36- S. T. Merlino, F. Sartori, The structures of m-cyanoaniline and p-cyanoaniline, Acta Crystallographica Section B: Structural Crystallography and Crystal Chemistry, **1982**, 38(5), 1476-1480.
37- G. Delgado, A. J. Mora, Crystal structure determination of p-bromoaniline using laboratory X-ray powder diffraction data, Materials Science Forum. Transtec Publications, **2001**, 378(2), 795-797.
38- G. Ploug-Sørenson, E. K. Andersen, Structure determination of p-chloroaniline hydrochloride, $C_6H_7ClN^+.Cl^-$, and redetermination of p-chloroaniline, C_6H_6ClN, Acta Crystallographica Section C: Crystal Structure Communications, **1985**, 41(4), 613-615.
39- D. G. Lister, J. K. Tyler, J. H. Høg, N. W. Larsen, The microwave spectrum, structure and dipole moment of aniline, Journal of Molecular Structure, **1974**, 23(2), 253-264.
40- G. Schultz, G. Portalone, F. Ramondo, A. Domenicano, I. Hargittai, Molecular structure of aniline in the gaseous phase: A concerted study by electron diffraction and ab initio molecular orbital calculations, Structural Chemistry, **1996**, 7(1), 59-71.
41- G. Roussy, A. Nonat, Determination of the equilibrium molecular structure of inverting molecules by microwave spectroscopy: application to aniline, Journal of Molecular Spectroscopy, **1986**, 118(1), 180-188.
42- M. A. Palafox, M. Gill, N. J. Nunez, V. K. Rastogi, L. Mittal, R. Sharma, Scaling factors for the prediction of vibrational spectra. II. The aniline molecule and several derivatives, International journal of quantum chemistry, **2005**, 103(4), 394-421.
43- A. Hastie, D. G. Lister, R. L. McNeil, J. K. Tyler, Substituent effects in benzene: the microwave spectrum of p-fluoroaniline, Journal of the Chemical Society D: Chemical Communications, **1970**, (2), 108-109.
44- Larsen NW, Hansen EL, Nicolaisen FM. Far infrared investigation of aniline and 4-fluoroaniline in the vapour phase. Inversion and torsion of the amino group, Chemical Physics Letters, **1976**, 43(3), 584-586.
45- E. Klein, V. Lukeš, Z. Cibulková, J. Polovková, Study of N–H, O–H, and S–H bond dissociation enthalpies and ionization potentials of substituted anilines, phenols, and thiophenols, Journal of Molecular Structure: THEOCHEM, **2006**, 758(2-3), 149-159.
46- G. Fronza, R. Mondelli, F. Lelj, E. W. Randall, C. A. Veracini, Structural changes induced in the NH_2 group of aniline by substituents: The structure and orientation of para-bromo-and para-nitroaniline [1-15N] in nematic liquid crystal solvents by NMR, Journal of Magnetic Resonance (1969), **1980**, 37(2), 275-284.
47- S. F. Mason, 723. The frequencies and intensities of the N–H stretching vibrations in primary amines, Journal of the Chemical Society (Resumed), **1958**, 3619-3627.
48- M. Haeberlein, J. S. Murray, T. Brinck, P. Politzer, Calculated electrostatic potentials and local surface ionization energies of para-substituted anilines as measures of substituent effects, Canadian Journal of Chemistry, **1992**, 70(8), 2209-2214.
49- P. J. Krueger, H. W. Thompson, Vibrational band intensities in substituted anilines, Proceedings of the Royal Society of London. Series A. Mathematical and Physical Sciences, **1957**, 243(1233), 143-153.
50- D. V. Kumar, V. A. Babu, G. R. Rao, G. C. Pandey, Vibrational analysis of substituted anilines, anisoles and anisidines: Part I. Vibrational spectra and normal coordinate analysis of some nitro compounds, Vibrational Spectroscopy, **1992**, 4(1), 39-57.
51- A. H. Yateem, Rotational Barrier and Conjugation: Theoretical Study of Resonance Stabilization of Various Substituents for the Donors NH_2 and OCH_3 in Substituted 1, 3-Butadienes, Indonesian Journal of Chemistry, **2019**, 19(4), 1055-1065.